

Magnetic susceptibility studies of the spin-glass and Verwey transitions in magnetite nanoparticles

K. L. López Maldonado, P. de la Presa, E. Flores Tavizón, J. R. Farias Mancilla, J.A. Matutes Aquino, A. Hernando Grande, and J.R. Elizalde Galindo.

Abstract

Magnetite nanostructured powder samples were synthesized by aging chemical method. Phase, structural, and magnetic properties were characterized. X-ray diffraction patterns showed cubic magnetite pure phase, with average crystallite size, $\langle D \rangle$, equal to 40 nm. Susceptibility measurements showed the well-known Verwey transition at a temperature of 90 K. The decrease of Verwey transition temperature, with respect to the one reported in literature (125 K) was attributed to the low average crystallite size. Moreover, the spin-glass like transition was observed at 35 K. Activation energy calculated from susceptibility curves, with values ranging from 6.26 to 6.93 meV, showed a dependence of spin-glass transition on frequency. Finally, hysteresis loops showed that there is not an effect of Verwey transition on magnetic properties. On the other hand, a large increase of coercivity and remanent magnetization at a temperature between 5 and 50K confirmed the presence of a magnetic transition at low temperatures.

Introduction

Even though magnetite has been studied since the beginning of magnetism, nowadays it is a material under unceasing study because of its exciting physical



properties; where its ferrimagnetic and half-metal characters give a strong interest to be applied in spintronic devices, letting to possibilities in applications on innovative technology that is in constant development.¹ One more attractive characteristic in magnetite is that it presents two particular and interesting low temperature transformations.²⁻⁵ The most known and studied is the one occurring around 120 K, called as its discoverer, Verwey, whom first reported it in 1939. When going below Verwey transition temperature, T_V , a change in crystalline structure takes place from cubic to monoclinic, leading to a decrease of 2 orders of magnitude in its electrical resistance. The origin of this drop in electrical resistance is still under discussion, but it is assumed that there occurs a charge order-disorder transition in crystal structure.⁶⁻⁸ the other interesting transformation in magnetite is the so called spin-glass transition, where a transition from high temperature ferromagnetic state to low temperature paramagnetic state happens at the grain surfaces. This is, below temperature of spin-glass transition, T_{sg} , grain-boundary spins freeze, and a drop in magnetization would take place.^{1,5,9}

The better understanding of these two transitions will be crucial to increase the possibility to found applications for this material in spintronic devices.^{1,10} In this way, this work presents the temperature behavior of susceptibility and hysteresis of Fe_3O_4 nanoparticles.

Experimental methodology

Magnetite nanoparticles were obtained by mixing an oxidant and a ferrous solution, as described by Vergés et al.¹¹ During synthesis, ferrous solution containing



Fe_2SO_4 0.34M and H_2SO_4 10^{-1} M was added to the oxidant solution containing KNO_3 and NaOH, with concentrations of 7×10^{-2} and 10^{-1} M, respectively. The solutions were mixed under N_2 atmosphere; after 5 min of reaction, the mixed solution was left to an aging procedure. The solution was aged during 120 min at 563K under constant magnetic stirring regime. After, the precipitated formed was washed several times and left to overnight dry.

The dried powder was then characterized by X-ray diffraction (XRD) in a PANalytical X'PertPro MPD diffractometer and by SEM in a field emission microscope JSM7000F; these two characterizations to observe microstructural properties such as phase purity, crystallite, and particle size. Magnetic properties were observed, first by susceptibility measurements carried out in an Oxford Instruments Susceptometer. Susceptibility charts were measured in a temperature range of 5 to 150K with $\Delta T=5$ K, and frequencies varying from 100 to 1291 Hz and under an applied magnetic field of $H_{ac}=50$ Oe. Finally, magnetic hysteresis loops were measured with a maximum applied field of $H=20$ kOe and in a temperature range from 5 to 300 K. Results from characterization were analyzed in order to have a good understanding on the transformations observed in magnetite nanoparticles at low temperatures.



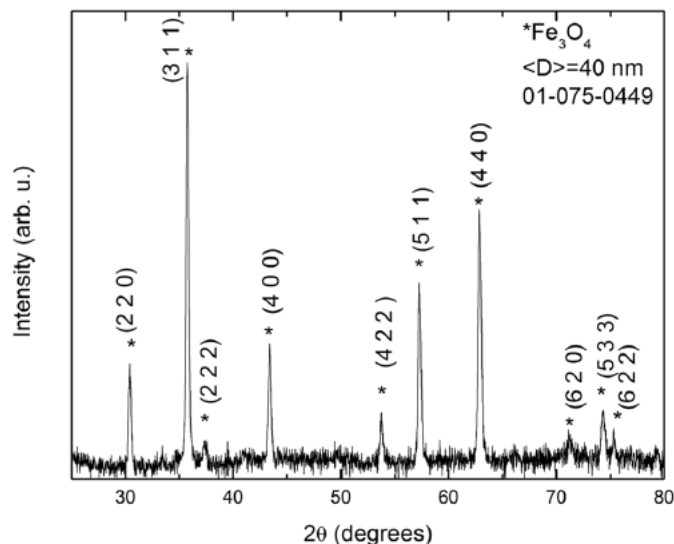


FIG. 1. X-ray diffraction pattern for Fe_3O_4 nanoparticles with $\langle D \rangle = 40$ nm.

Results and discussion

Figure 1 shows XRD diffraction pattern obtained for the Fe_3O_4 nanoparticles. The sample was identified and indexed with the pure magnetite cubic crystalline phase (#PDF01-075-0449). During analysis, no secondary phase was observed. Using Scherrer's formula, and taking FWHM of (311) peak, average crystallite size was found to be $\langle D \rangle = 40$ nm. Cell parameter was calculated using UNITCELL software,¹² obtaining values of $a = 8.35 \text{ \AA}$.

Figure 2 shows in-phase susceptibility measurements of the Fe_3O_4 nanoparticles. Here, two slope changes at low temperatures were observed, indicating two different transitions. The first was identified as the Verwey transition. Owing to this transition is a crystallographic transformation, the order and rearranging of the atoms during and after transformation are going to affect the electronic distribution and, therefore, the magnetic alignment of spins. This is observed as a little slope change in magnetic susceptibility

curves at TV. Verwey transition is reported by several authors to have values around 120K for bulk samples,^{1,5,8-10} but, for our nanoparticles, it decreases to 90 K. Using an elementary thermodynamic model, this reduction can be associated to an increment on surface energy due to the small crystallite size, leading to a reduction of the energy barrier for the transformation to occur; hence, a reduction on the transition temperature befalls because of the size of nanocrystals.¹³

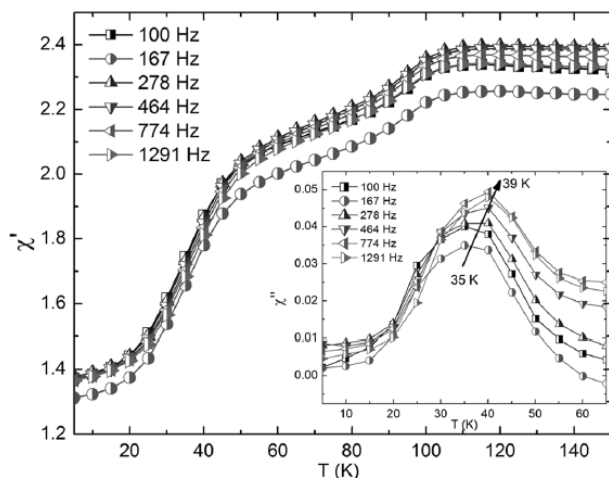


FIG. 2. Fe_3O_4 nanoparticles in-phase susceptibility curves for temperature ranging from 5 to 150 K. At the inset, out-phase susceptibility curves; the peak shifting with frequency is pointed.

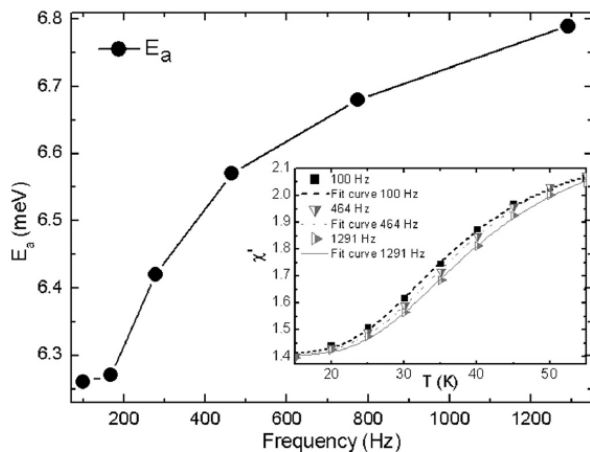


FIG. 3. Activation energy, E_a , dependence on frequency. The inset shows the in-phase susceptibility curves with their corresponding fittings.

The second transition observed at lower temperature, $T_{sg}=35$ K, was a spin-glass like, which could be seen in both the in-phase and out-phase susceptibility curves (Fig. 2). As seen at the inset on Figure 2, at the out-phase curves, a peak shift was observed for the T_{sg} for the higher frequencies. To reach a deeper understanding of this behavior, and using inphase curves, the activation energy, E_a , necessary for the spinglass to be broken was calculated from the Cole and Cole generalized Debye relaxation mechanism, which describes the response of susceptibility as $X_{AC} \propto X_{AC}/(1+i\omega\tau)$, and from its relationship with relaxation time that follows $\tau=\tau_0\exp(E_a/k_B T)$.⁵ The values obtained for the E_a and τ are shown in Table I. It can be observed that E_a and τ are frequency dependent, as correspond to the observed peak-shifting of T_{sg} in out-phase curves. Figure 3 shows the above mentioned dependence of E_a on frequency. To illustrate the fittings used to calculate the activation energy, E_a , the inset shows the susceptibility data sets of three selected frequencies and their corresponding fitting curves. This behavior could be, partially, attributed to the Fe_3O_4 nanoparticles crystallite size distribution which affects the magnitude of disordered surface area; but this is still under discussion.¹⁴⁻¹⁶

Finally, because the spin-glass is a magnetic transition, when spin-glass transition occurs at the grain surface, the surface magnetic anisotropy at the grain would significantly increase, leading to an increment in coercivity at the T_{sg} due to the strong coupling between the ordered spins inside the grain and the disordered spins at the surface.⁹



TABLE I. Activation energy, E_a , and relaxation time, τ , calculated from magnetic susceptibility curves for the different frequencies.

Frequency (Hz)	τ (s)	E_a (meV)
100	$2.35 \times 10^{-4} \pm 4.45 \times 10^{-5}$	6.26 ± 0.48
167	$1.48 \times 10^{-4} \pm 3.00 \times 10^{-5}$	6.27 ± 0.50
278	$8.69 \times 10^{-5} \pm 1.48 \times 10^{-5}$	6.42 ± 0.44
464	$5.05 \times 10^{-5} \pm 9.35 \times 10^{-6}$	6.57 ± 0.50
774	$2.98 \times 10^{-5} \pm 5.87 \times 10^{-6}$	6.68 ± 0.52
1291	$1.77 \times 10^{-5} \pm 3.64 \times 10^{-6}$	6.79 ± 0.56

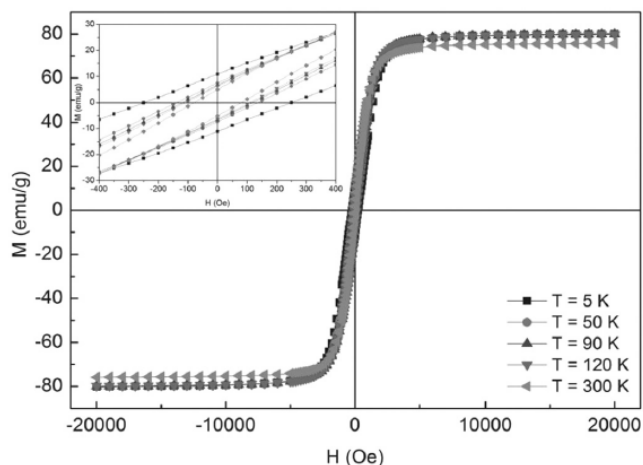


FIG. 4. Hysteresis loops for Fe_3O_4 nanoparticles at different temperatures. At the inset, a zoom to the coercivity values, where a big decrease on coercivity confirmed the spin-glass transition.

To probe this, Figure 4 shows the hysteresis loops measured at temperatures of 5, 50, 90, 120, and 300 K. The inset shows that coercivity decreases to almost half its value when temperature goes from 5 to 50K. This decrement at low temperatures ratifies the presence of a spin-glass transition in the Fe_3O_4 nanoparticles.

Conclusions



Single phase Fe₃O₄ nanoparticles with $\langle D \rangle = 40$ nm were obtained by aging chemical method. Susceptibility measurements and analysis exposed the Verwey and Spin-glass transitions, with temperatures $T_V = 90$ K and $T_{sg} = 35$ K, respectively. The reduced values of Verwey transition temperature were attributed to the small average crystallite size and with this, the increment of surface energy. The analysis of activation energy associated to the observed spin-glass like behavior exposed a T_{sg} dependent on frequency; which, in addition to the large increment in coercivity values at low temperatures, confirms the presence of a spin-glass transition in the Fe₃O₄ nanoparticles.

Acknowledgments

The authors would like to acknowledge UACJ, CIMAV, and IMA for the support given to this research.

References

1. M. Balanda, A. Wiechec, D. Kim, Z. Kakol, A. Kozlowski, P. Niesiela, and J. Sabol, Eur. Phys. J. B 43, 201 (2005).
2. J. Garcia and G. Subias, J. Phys.: Condens. Matter 16, R145 (2004).
3. D. J. Huang, H. J. Lin, J. Okamoto, K. S. Chao, H. T. Jeng, G. Y. Guo, C. H. Hsu, C. M. Huang, D. C. Ling, W. B. Wu, C. S. Yang, and C. T. Chen, Phys. Rev. Lett. 96, 096401 (2006).
4. R. H. Kodama, A. E. Berkowitz, E. J. McNiff, and S. Foner, Phys. Rev. Lett. 77, 394 (1997).
5. Z. Janu, J. Hadac, and Z. Svindrych, J. Magn. Magn. Mater. 310, e203



(2007).

6. P. Brahma, S. Dutta, S. Banerjee, A. Ghosh, and D. Chakravorty, *J. Magn. Mater.* 321, 1045 (2009).

7. A. Pimenov, S. Tachos, T. Rudolf, A. Loidl, D. Schrupp, M. Sing, R. Claessen, and V. A. M. Brabers, *Phys. Rev. B* 72, 035131 (2005).

8. P. Poddar, T. Fried, G. Markovich, A. Sharoni, D. Katz, T. Wizansky, and O. Millo, *Europhys. Lett.* 64 (1), 98 (2003).

9. Z. L. Lu, W. Q. Zou, L. Y. Lv, X. C. Liu, S. D. Li, J. M. Zhu, F. M. Zhang, and Y. W. Du, *J. Phys. Chem. B* 110, 23817 (2006).

10. W. B. Mi, J. J. Shen, E. Y. Jiang, and H. L. Bai, *Acta Mater.* 55, 1919 (2007).

11. A. Vergés, M. R. Costo, A. G. Roca, J. F. Marco, G. F. Goya, C. J. Serna, and M. P. Morales, *J. Phys. D: Appl. Phys.* 41(13), 134003 (2008).

12. T. J. B. Holland and S. A. T. Redfern, *Miner. Mag.* 61, 65 (1997).

13. J. C. Niépce and L. Pizzagalli, "Structure and phase transitions in nanocrystals,"

in *Nanomaterials and Nanochemistry*, edited by C. Brécheignac,

P. Houdy, and M. Lahmani (Springer-Verlag, Berlin, 2007), pp. 35–54.

14. P. Dey, T. K. Nath, P. K. Manna, and S. M. Yusuf, *J. Appl. Phys.* 104, 103907 (2008).

15. K. Trachenko, *J. Phys.: Condens. Matter* 23, 366003 (2011).



<https://cimav.repositorioinstitucional.mx/jspui/>

16. M. Castellana, A. Decelle, and E. Zarinelli, Phys. Rev. Lett. 107, 275701 (2011).

